Available online at www.sciencedirect.com

ScienceDirect

Procedia Computer Science 37 (2014) 293 – 300

Procedia Computer Science

The 4th International Conference on Current and Future Trends of Information and Communication Technologies in Healthcare (ICTH-2014)

# An Approach for Efficient Detection of Cephalometric Landmarks

Thuong Le-Tien, Hieu Pham-Chi*

*Ho Chi Minh city University of Technology, Ho Chi Minh city 70000, Vietnam*

**Abstract**

In this paper, a method is developed for the automated identification of cephalometric landmarks in orthodontics. The process of soft tissue edge detection is divided into two steps: detecting the sub-images that contained the required landmarks using combination of the Histograms of Oriented Gradients (HOG) descriptor with the Support Vector Machine (SVM), then utilizing Thresholding and Mathematical Morphological (TMM) algorithm to trace soft tissue profile. In addition, the mandible's edge is detected by the Active contours without edges (Chan-Vese method). Finally, the landmarks of soft tissue profile and the mandible's edge are pinned based on analyzing the contour plot of these lines. The simulation results have high accuracy.


Peer-review under responsibility of the Program Chairs of EUSPN-2014 and ICTH 2014.

*Keywords:* Cephalometric Landmarks; Histograms of Oriented Gradients; Support Vector Machine; Thresholding and Mathematical Morphological; Active contours without edges.

## 1. Introduction

Cephalometry is the analysis of the dental and skeletal relationships in the head between bony and soft tissue landmarks [18]. The cephalometric analysis is widely used in orthodontics to diagnose facial growth abnormalities and plan treatment. Up to now, the allocation of cephalometric landmarks manually on X-ray images is a time-consuming process and can be affected by errors despite of an experienced surgeon. Consequently, many researchers have tried to automate landmark allocation for many years.

Levy-Mandel et al. [1] introduced the first work of automated location of cephalometric landmarks in 1986. However, they did not compare their results of detecting landmarks on two high quality images to the manual identification. Some researchers used the knowledge-based techniques or image matching methods, and then

* Corresponding author. Tel.: +84 903 787 989.
*E-mail address:* thuongle@hcmut.edu.vn


Peer-review under responsibility of the Program Chairs of EUSPN-2014 and ICTH 2014.
doi:10.1016/j.procs.2014.08.044

learning systems. Parthasarathy et al. [2] improved the method of Levy-Mandel by including a pyramid resolution with four levels to increase the speed of system in 1989. The methods using similar knowledge-based technique are presented in [3], [4], [5], [6], [7]. Later, Cardillo et al [8] used mathematical modeling and a pattern matching technique to localize landmarks. Grau et al. [9] have developed the previous work using a model of the edge detection, then applying a pattern detection algorithm based on mathematical morphology techniques. Then, Rudolph [10] used the knowledge of the spatial spectroscopy which establishes a statistical model gray assumes a special statistical highlight of each landmark in different images. In addition, Uchino et al. [11] presented a fuzzy learning machine that could learn the relationship between the value of average gray level of an entry and the location of the landmark. In 1999 Chen et al. [12] used neural networks and genetic algorithms to find sub-images that contain cephalometric points. El-Feghi et al. [13] applied neuro-fuzzy network and a template-matching technique. Poyan et al. [14] used the Histograms of Oriented Gradients to describe sub-images which have landmarks and the Support Vector Machine to identify. But this method consumes time by SVM-Light [15]. Moreover, Mohseni et al [16] identified 8 landmarks with high accuracy based on the similarities in human anatomical structure and form an affine transform, and template matching schemes. Besides, Favaedi et al. [17] presented a methodology to locate the landmarks based on probabilistic relaxation. Their method depends on a reference shape template which formatted previously, is quite similar to the soft tissue profile surrounding the nose. In the surveying, many researchers interest in the cephalometry and have a lot of methods but there is not any standard for this topic. This work does not discuss about the comparison and their disadvantages, just contributes a new efficient method to solve the theme.

Table 1. Twelve soft tissue landmarks and their definitions [18].

| No. | Landmark | Definition |
|---|---|---|
| 1 | Soft tissue Glabella' (G') | The most prominent point of the forehead on the midsagittal plane at the superior aspect of the eyebrows. |
| 2 | Soft tissue Nasion (Na') | The outer point of intersection between the Nasion horizontal line and the soft tissue. |
| 3 | Pronasale (P) | The tip of the nose. |
| 4 | Subnasale (Sn) | The junction of the nose to the upper lip. |
| 5 | Soft tissue A point (A') | The outer point of intersection between the A point horizontal line and the soft tissue. |
| 6 | Upper Lip Anterior (ULA) | The most anterior extension of the upper lip at the vermilion border. |
| 7 | Stomion (St) | The junction of the upper to lower lip. |
| 8 | Lower Lip Anterior (LLA) | The most anterior extension of the lower lip at the vermilion border. |
| 9 | Soft tissue B point (B') | The outer point of intersection between the B point horizontal line and the soft profile. |
| 10 | Soft tissue Pogonion (Pg') | The outer point of intersection between the Pogonion horizontal line and the soft profile. |
| 11 | Soft tissue Menton (Me') | The outer point of intersection between the Menton vertical line and the soft tissue. |
| 12 | Soft tissue Gnathion (Gn') | The midpoint of soft tissue Pogonion' and soft tissue Menton'. |

Table 2. Four landmarks on the mandible's edge and their definitions [25].

| No. | Landmark | Definition |
|---|---|---|
| 1 | Point B (B) | The most posterior point on the profile of the mandible between the chin point and the alveolar crest |
| 2 | Pogonion (Pg) | The most anterior point on the bony chin. |
| 3 | Menton (Me) | The most inferior point on the chin in the lateral view. |
| 4 | Gnathion (Gn) | The midpoint of Pogonion and Menton. |

Soft tissue profile analysis from cephalometric radiographs is recognized as an important process of the assessment of treatment outcome in cleft lip and palate, and used to distinguish between groups better than conventional hard tissue cephalometric analysis. Holdaway et al. [18] introduced first methods of cephalometric soft tissue analysis within definitions of landmarks. Twelve soft-tissue landmarks and four landmarks on the mandible's edge are discussed in this article. All of them are significant in successful orthodontic outcome, and none of them

depend on skeletal landmarks for measurement. Table 1 and table 2 respectively shows the definitions of twelve soft tissue landmarks and four landmarks on the mandible's edge.

## 2. Automatic localization of soft tissue cephalometric landmarks.

This paper proposes an approach to localize automatically twelve soft tissue landmarks shown in Fig.1 (a). Firstly, the linear Support Vector Machine trains a set of templates which extract the Histograms of Oriented Gradients of the desired points [19], then recognizes patterns and localizes these areas on the input image shown in Fig.1 (b). The method from paper [19] is modified and developed more for the soft tissue. Secondly, the soft tissue profile is extracted from a background of noise and irrelevant lines by the Thresholding and Mathematical Morphological algorithm. Finally, from analyzing the contour plot of the traced profile, the relatively accurate landmarks are figured out. A flowchart of this process is summarized in the Fig.2.

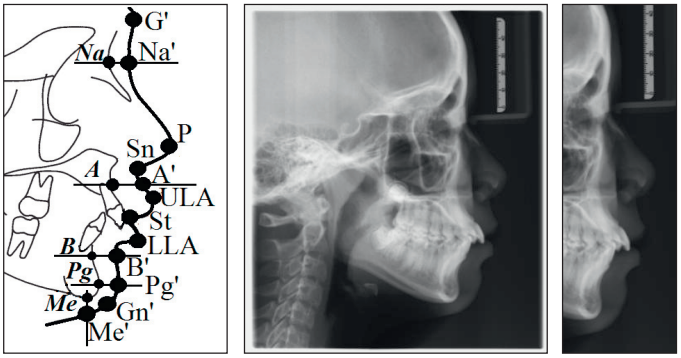


Fig.1. (a) Localization of twelve soft tissue landmarks. (b) An input image. (c) The zoom version of soft tissue profile region.

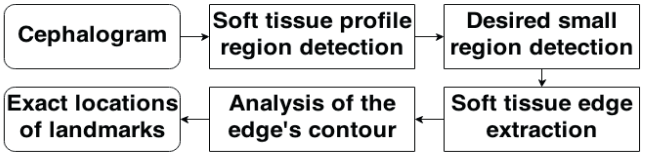


Fig.2 . The flowchart of the proposed method.

### *2.1. Detecting soft tissue profile region.*

In this step, we propose the method based on the use of HOG descriptor [20] and a non-probabilistic binary linear classifier SVM to detect the soft tissue profile of the input image. The reference model is based on samples contained the HOG feature of nose image similar to the Fig.1(c) and trained by the libSVM [21] classifier. The configurations of SVM training for regression (epsilon-SVR) are a linear Gaussian kernel, a soft margin parameter 0.5, the epsilon setting in loss function 0.5 and the tolerance of termination criterion setting 0.5. To reduce total execution time, the input image and the training templates should be scaled down by the same appropriate rate $\beta_1$ which is experienced gradually is not lower than 1/10. After that, the one-class libSVM predicts and decides the most exact detection of the soft tissue profile image. Its first location of the image matrix is multiplied by the rate $\beta_1$ and then the input is cropped with this coefficient in order to remove irrelevant and unnecessary details.

### *2.2. Detecting desired small region.*

Similarly, the combination of HOG and SVM searches again four desired smaller regions from the soft tissue profile image including the forehead, the nose, the lip and the mandible. The resolutions of these region should be

suitable for the strategy of each area which is presented in Section Analysis of the edge's contour so that the images contain the important landmarks. The input and the samples, the trained images, are scaled down with the rate $\beta_2$ of 0.8. After finding the locations of each small image and multiplying with $\beta_2$, the output is cropped from the soft tissue image. The Fig.3 (a),(f),(k) and (p) shows recognition results of the desired small areas whose real resolutions are different corresponding to 600x300, 400x300, 400x300 and 400x400 pixels.

*2.3. Soft tissue edge extraction.*

After detecting the small regions, the soft tissue edge needs to be traced by Thresholding and Mathematical Morphological (TMM) algorithm. The famous thresholding method of Otsu [22] is effective for skeletal edges, shown in Fig.3 (b), (g), (l) and (q). However, the aim of extraction is the soft tissue edge. Thresholding after histogram equalization does not identify correctly total desired edges and incurs irrelevant edges. Therefore, after the histogram equalization, we propose that these input images should be adjusted with an intensity value α [22]. This factor specifies the shape of the curve which describes a relationship between values in the input image and its output. Several experiments show that each region has a different value presented in Fig.3. The factor α is generally less than 1, the mapping is weighted toward higher output values. These outputs are converted to binary images based on threshold of 0.5. After that, the Mathematical Morphology process removes small extra regions and holes from the binary images. The useful edge of soft tissue is highlighted and isolated to detect exact landmarks.

*2.4. Analysis of the edge's contour.*

In the section, according to the definition of each landmark, a proper technique is used to accurate its location. Assume that coordinates of two important skeletal landmarks: point Nasion (Na) and point A which have detected before are the basis for soft tissue points. It must be noticed that this method also can detects three skeletal landmarks: point B, Pogonion (Pg) and Menton (Me), however, its locations just be reference points, not the soft tissue landmarks. Four representations of contour's soft tissue profile of the forehead, the nose, the lip and the mandible shown in Fig. 3 correspond to $f_1(x)$, $f_2(x)$, $f_3(x)$ and $f_4(x)$. These contours are the approximated edges that are detected in the previous subsection. O$x$ and O$y$ are respectively the horizontal and vertical axes with the pixel unit. The following equations based on the definitions perform exactly how to find the desired landmarks from these contours.

The point Soft tissue Glabella' (G') is the point of the contour $f1(x)$ at which the value of x coordinate is the largest ($x_{1max}$) within its y-value less than point Nasion's vertical value:

$$G'(x_{G'} = x_{1max}, y_{G'} = f_1(x_{1max})) \qquad \forall\, y < y_{Na} \tag{1}$$

The x-value of the Nasion (Na) and Soft tissue Nasion' (Na') point is the same, so:

$$Na'(x_{Na'} = f_1^{-1}(y_{Na}), y_{Na'} = y_{Na}) \tag{2}$$

The Point Pronasale $Pg'(x_{Pg'}, y_{Pg'})$ by the contour $f_2(x)$ without conditions is similar to Point A. $x_{2max}$ is the maximum x-value of the contour of $f_2(x)$. This point can be defined to be:

$$P(x_P = x_{2max}, y_P = f_2(x_{2max})) \tag{3}$$

After the coordinate of point P, the point Subnasale (Sn) has the minimum x-value $x_{2min}$ of the contour $f_2(x)$:

$$Sn(x_{Sn} = x_{2min}, y_{Sn} = f_2(x_{2min})) \qquad \forall\, y_P < y < y_A \tag{4}$$

To locate the point Upper Lip Anterior (ULA), the point Stomion (St) and the point Lower Lip Anterior (LLA) by the contour $f_3(x)$, the point St is calculated firstly and then the points ULA and LLA within point St's conditions:

$$St(x_{St} = x_{3\min}, y_{St} = f_3(x_{3\min})) \tag{5}$$

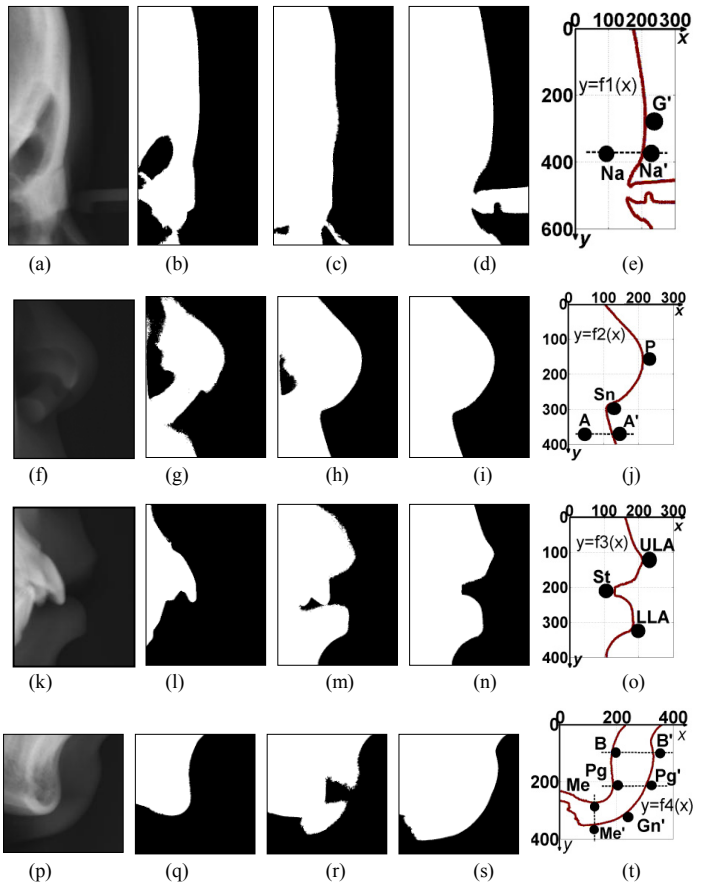


Fig.3. Soft tissue edge extraction of the desired small regions. (a): The forehead. (f): The nose. (k): The lip. (p): The mandible. (b),(g),(l),(q): Thresholding by Otsu method. (c),(h),(m),(r): Thresholding a value of 0.5 after histogram equalization. (d),(i),(n),(s): The proposed thresholding and mathematical morphology. (e),(j),(o),(t): Analyzing the contours of soft tissue profiles edges.

The points ULA and LLA have the same calculation but with two different planes: the y-value of ULA is less than the St's while the LLA's is greater. Here, $x_{3max}$ and $x_{3min}$ are respectively the maximum and minimum x-value of the contour of $f_3(x)$:

$$ULA(x_{ULA} = x_{3max}, y_{ULA} = f_3(x_{3max})) \qquad \forall\, y < y_{St} \tag{6}$$

$$LLA(x_{LLA} = x_{3max}, y_{LLA} = f_3(x_{3max})) \qquad \forall\, y < y_{St} \tag{7}$$

The y-value of the point Menton (Me) and the point Soft tissue Menton' (Me') by the contour $f_4(x)$ is the same:

$$Me'(x_{Me'} = x_{Me}, y_{Me'} = f_4(x_{Me})) \tag{8}$$

The point Soft tissue Gnathion $Gn'(x_{Gn'}, y_{Gn'})$ is the midpoint of soft tissue Pogonion' and soft tissue Menton'. From this definition, the length of the curve Arc length L(Me'Gn') is the same as Arc length L(Gn'Pg'):

$$L(Me'Gn') \approx L(Gn'Pg') \tag{9}$$

Hence, the method of locations of points A', B' and the point Soft tissue Pogonion (Pg') is similar to the point Na' represented in equation (2). To access the placement of the landmarks, the paper applied this method to a number of cephalograms and compared the manually detected position of the landmarks with those automated identification. Following the discussion in [23], the distance of error less than 2 mm is considered acceptable. The percentage of automatically detected landmarks based on the proposed algorithm is shown in Table 3.

Table 3: Experiment Results.

| Resolution | No. of Images | ± 2mm (pixels) | ≤ 2mm of error (%) |
|---|---|---|---|
| 1840x1360 | 40 | ≈ 16 | 75.00 |
| 2012x1735 | 30 | ≈ 16 | 88.89 |
| 2136x1804 | 80 | ≈ 21 | 76.04 |

## 3. Detection of the landmarks on the mandible's edge using the Active contours without edges.

This section proposes an approach to localize automatically four soft tissue landmarks on the mandible's edge. An active contour model, often called snake in the literature, is a dynamic structure used in image processing and computer vision. Several approaches are possible and solve the problem of segmentation and edge detection using a deformable curve model that conforms to the shape of objects. The contour C and the values $\mu_{in}$, $\mu_{out}$ that are shown in Fig.4 minimize the following energy functional:

$$F(C, \mu_{in}, \mu_{out}) = \int \Omega_{in} (\mu_{in} - I_0)^2 dxdy + \int \Omega_{out} (\mu_{out} - I_0)^2 dxdy + \nu \int_C ds \tag{10}$$

Where F is the energy functional, $I_0$ is the input image, $\mu_{in}$, $\mu_{out}$ and $\nu$ are constant parameters larger than 0. The function of contour is used to make automatically topology changes and solved by the Euler-Lagrange equation and the Heaviside function H. Finally, these results $\mu_{in}$ and $\mu_{out}$ are the active contour model without edges [24]:

$$\mu_{in} = \frac{\int_\Omega I_0 H(\phi) dxdy}{\int_\Omega H(\phi) dxdy}; \mu_{out} = \frac{\int_\Omega I_0 (1 - H(\phi)) dxdy}{\int_\Omega (1 - H(\phi)) dxdy} \tag{11}$$

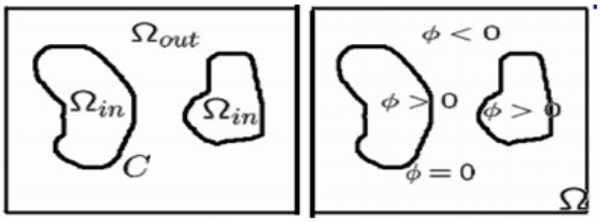


Fig.4. Propagation in the normal direction of the contour C.

### 3.1. Detecting the edge of the mandible.

Similarly, the combination of HOG and SVM searches the most accurate sub-region which contains the mandible's edge. After that, the algorithm Chan-Vese [24] will cling to the edge of the mandible and approximate its

contour. The experiment shows the expected edge that is detected after 700 times shown in Fig.5 (a). (b). Then, Mathematical Morphological algorithms remove small extra regions to perform one representations of contour *y=f(x)*, where the horizontal and vertical axes are Ox and Oy.

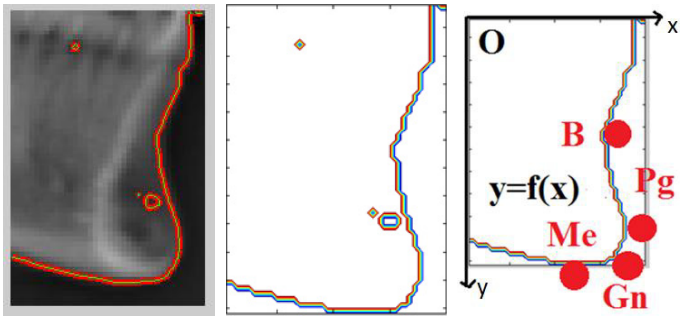


Fig.5. (a) A result of detection of the landmarks on the mandible using the Active contours without edges. (b) The contour of the mandible's edge. (c) Analyzing the contours of the mandible's edges.

*3.2. Localization of the landmarks on the mandible's edge.*

From the definitions of landmarks in Table 2, the points $B(x_B, y_B)$, Pogonion $Pg(x_{Pg}, y_{Pg})$, Menton $Me(x_{Me}, y_{Me})$ will be calculated from these equations (12), (13) and (14):

$$B(x_B = x_{\min}, y_B = f(x_{\min})) \qquad \forall\, y < y_{Pg} \tag{12}$$

$$Pg(x_{Pg} = x_{\max}, y_{Pg} = f(x_{\max})) \qquad \forall\, y > y_B \tag{13}$$

$$Me(x_{Me} = f^{-1}(y_{\max}), y_{Me} = y_{\max}) \tag{14}$$

Where $x_{\min}$ and $x_{\max}$ are respectively the minimum and maximum x-value of the representations of contour *y=f(x)*, and $y_{\max}$ is maximum y-value. The same as the point soft tissue Gn', the point Gnathion $Gn(x_{Gn}, y_{Gn})$ on the mandible's edge be inferred from the length of the curve Arc length $L(MeGn)$ and $L(GnPg)$:

$$L(MeGn) \approx L(GnPg) \tag{15}$$

**4. Conclusion.**

In this work, the authors have a new method for the extraction of soft tissue landmarks and landmarks on mandible's edge in cephalometry. A technique based on the combination of HOG descriptor and SVM learning limits the search regions that contained desired features through two steps. The soft tissue profile is extracted by the TMM algorithm; while the mandible's edge is extracted by the Active contours without edges, and then they are analyzed and calculated to pin points by the definitions. The landmarks are identified with accuracy comparable and fast execution time. But there also are some limits of our approach. One is about the intensity value α which inferred from the limited number of input image. The value of α can be exactly calculated from a large dataset of cephalograms. The second limitation is related to number of input image in the experiment results. The source of cephalometric images is poor because of the individual rights. Our future work will solve these two problems.

**Acknowledgements:**

The authors appreciate the NAFOSTED (the National Foundation for Science and Technology Development in Vietnam) for their financial support to present the work at the conference.

**References:**

1. A. Levy-Mandel, A. Venetsanopoulos, and J. Tsotsos, "Knowledge-based landmarking of cephalograms," Computers and Biomedical Research, vol. 19, no. 3, pp. 282–309, 1986.
2. S. Parthasarathy, S. Nugent, P. Gregson, and D. Fay, "Automatic landmarking of cephalograms," Computers and Biomedical research, vol. 22, no. 3, pp. 248–269, 1989.
3. D. N. Davis and D. Forsyth, "Knowledge-based cephalometric analysis: a comparison with clinicians using interactive computer methods," Computers and Biomedical research, vol. 27, no. 3, pp. 210–228, 1994.
4. C. Yan, A. Venetsanopoulos, and E. Fillery, "An expert system for landmarking cephalograms," in 6th Internation Workshop Vol. 1 on Expert Systems & Their Applications. Agence de l'Informatique, 1987, pp. 337–356.
5. P. Jackson, G. Dickson, and D. Birnie, "Digital image processing of cephalometric radiographs: a preliminary report." Journal of Orthodontics, vol. 12, no. 3, pp. 122–132, 1985.
6. J. D. Cohen, K. Dunbar, and J. L. McClelland, "On the control of automatic processes: a parallel distributed processing account of the stroop effect." Psychological review, vol. 97, no. 3, p. 332, 1990.
7. W. Tong, S. Nugent, G. Jensen, and D. Fay, "An algorithm for locating landmarks on dental x-rays," in Engineering in Medicine and Biology Society, 1989. Images of the Twenty-First Century., Proceedings of the Annual International Conference of the IEEE Engineering in. IEEE, 1989, pp. 552–554.
8. J. Cardillo and M. Sid-Ahmed, "An image processing system for locating craniofacial landmarks," Medical Imaging, IEEE Transactions on, vol. 13, no. 2, pp. 275–289, 1994.
9. V. Grau, M. Alcaniz, M. Juan, C. Monserrat, and C. Knoll, "Automatic localization of cephalometric landmarks," Journal of Biomedical Informatics, vol. 34, no. 3, pp. 146–156, 2001.
10. D. Rudolph, P. Sinclair, and J. Coggins, "Automatic computerized radiographic identification of cephalometric landmarks," American Journal of Orthodontics and Dentofacial Orthopedics, vol. 113, no. 2, pp. 173–179, 1998.
11. E. Uchino and T. Yamakawa, "High speed fuzzy learning machine with guarantee of global minimum and its application to chaotic system identification and medical image processing," International Journal on Artificial Intelligence Tools, vol. 5, no. 01n02, pp. 23–39, 1996.
12. [Y. J. Chen, S. K. Chen, H. F. Chang, and K. C. Chen, "Comparison of landmark identification in traditional versus computer-aided digital cephalometry," The Angle orthodontist, vol. 70, no. 5, pp. 387–392, 2000.
13. I. El-Feghi, M. A. Sid-Ahmed, and M. Ahmadi, "Automatic localization of craniofacial landmarks for assisted cephalometry," Pattern Recognition, vol. 37, no. 3, pp. 609–621, 2004.
14. A. A. Pouyan and M. Farshbaf, "Cephalometric landmarks localization based on histograms of oriented gradients," in Signal and Image Processing (ICSIP), 2010 International Conference on. IEEE, 2010, pp. 1–6.
15. T. Joachims, "Making large scale svm learning practical," 1999.
16. H. Mohseni and S. Kasaei, "Automatic localization of cephalometric landmarks," in Signal Processing and Information Technology, 2007 IEEE International Symposium on. IEEE, 2007, pp. 396–401.
17. L. Favaedi and M. Petrou, "Cephalometric landmarks identification using probabilistic relaxation." in Conference proceedings:... Annual International Conference of the IEEE Engineering in Medicine and Biology Society. IEEE Engineering in Medicine and Biology Society Conference, vol. 2010, 2009, pp. 4391–4394.
18. R. A. Holdaway, "A soft-tissue cephalometric analysis and its use in orthodontic treatment planning. part i," American journal of orthodontics, vol. 84, no. 1, pp. 1–28, 1983.
19. T. Le-Tien, T. Nguyen-Thien, H. Pham-Chi, T. Vuong-Duc, and P. Nguyen-Xuan, "Using the histogram of oriented gradients for detecting cephalometric landmarks," in Advanced Technologies for Communications (ATC), 2013 International Conference on. IEEE, 2013, pp. 580–585.
20. N. Dalal and B. Triggs, "Histograms of oriented gradients for human detection," in Computer Vision and Pattern Recognition, 2005. CVPR 2005. IEEE Computer Society Conference on, vol. 1. IEEE, 2005, pp.886–893.
21. C.-C. Chang and C.-J. Lin, "Libsvm: a library for support vector machines," ACM Transactions on Intelligent Systems and Technology (TIST), vol. 2, no. 3, p. 27, 2011.
22. R. C. Gonzalez, R. E. Woods, and S. L. Eddins, Digital image processing using MATLAB. Pearson Education India, 2004.
23. T. Rakosi and R. Meuss, An atlas and manual of cephalometric radiography. Wolfe Medical Publications London, 1982.
24. T. F. Chan and L. A. Vese, "Active contours without edges," Image processing, IEEE transactions on, vol. 10, no. 2, pp. 266–277, 2001.
25. Broadbent, B. Holly. "A new x-ray technique and its application to orthodontia: The introduction of cephalometric radiography." The Angle Orthodontist 51.2 (1981): 93-115.